

An optical study of the structure of the helicoidal twist grain boundary (TGB_A) phase

This article has been downloaded from IOPscience. Please scroll down to see the full text article.

1999 J. Phys.: Condens. Matter 11 1423

(<http://iopscience.iop.org/0953-8984/11/6/007>)

View [the table of contents for this issue](#), or go to the [journal homepage](#) for more

Download details:

IP Address: 171.66.16.214

The article was downloaded on 15/05/2010 at 06:58

Please note that [terms and conditions apply](#).

An optical study of the structure of the helicoidal twist grain boundary (TGB_A) phase

Richard J Miller^{†§}, Helen F Gleeson^{†||} and John E Lydon[‡]

[†] Department of Physics and Astronomy, University of Manchester, Manchester M13 9PL, UK

[‡] Department of Biochemistry and Molecular Biology, University of Leeds, Leeds LS2 9JT, UK

Received 18 September 1998, in final form 2 December 1998

Abstract. The optical properties of the liquid-crystal analogue of the Abrikosov phase, the TGB_A phase, have been examined for the first time using the Kossel technique. The Kossel diagrams observed between crossed polarizers each consist of a bright annulus on which a darker spiral pattern is superimposed. Identical patterns have been reported and explained previously for the chiral nematic phase and the results presented here indicate that the optics of the TGB_A phase are analogous to those of the cholesteric phase. Both the pitch and handedness of the TGB_A phase have been measured from the Kossel diagrams. The pitch of the material was found to be approximately linear with temperature, ranging from around 550 nm at the TGB_A -to- SmC_α^* phase boundary to 450 nm at the TGB_A -to-isotropic phase boundary.

1. Introduction

Kossel lines have an interesting history. Very early in the study of x-ray diffraction it was noticed that patterns of dark lines occurred in transmission photographs taken with divergent beams of monochromatic x-rays [1]. These were shadows of Bragg reflections and are formed as shown in figure 1. Since Bragg reflections occur in families of cones whose axes are normal to the reflecting planes, Kossel lines have the form of conic sections: circles, ellipses and hyperbolae, depending on the scattering geometry. The relative positions of Kossel lines can be very sensitive to the repeat distances in the sample and values for the unit-cell dimensions determined from them accurate to one part in 10^5 have been claimed.

Reflected x-ray Kossel lines, rather than their shadows, can also be observed, especially in situations where fluorescent x-rays are produced within the crystal. In the conventional geometry of x-ray diffraction studies, a collimated, approximately parallel beam of monochromatic radiation is used (figure 2(a)). The diffraction pattern given by a single crystal consists of an array of spots each of which corresponds to the Bragg reflection from a particular family of planes. If, however, the x-rays used have a wavelength close to an absorption edge of one of the atomic species present in the crystal, fluorescent x-rays are produced (figure 2(b)). Because this occurs within the crystal itself, the geometry of the diffraction effects is totally different. It can be treated as if there were a point source at the centre of the crystal. Patterns with a similar appearance are relatively common in electron diffraction studies and are known as Kikuchi lines.

[§] Present address: Merck Limited, Merck House, Poole, Dorset, UK.

^{||} Author to whom any correspondence should be addressed. E-mail address: helen.gleeson@man.ac.uk.

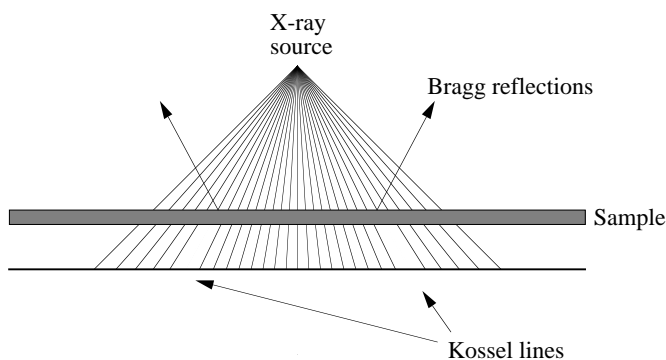


Figure 1. A representation of the first observations of Kossel lines as shadows in the pattern of transmitted x-rays, showing where Bragg reflection has weakened the transmitted beam.

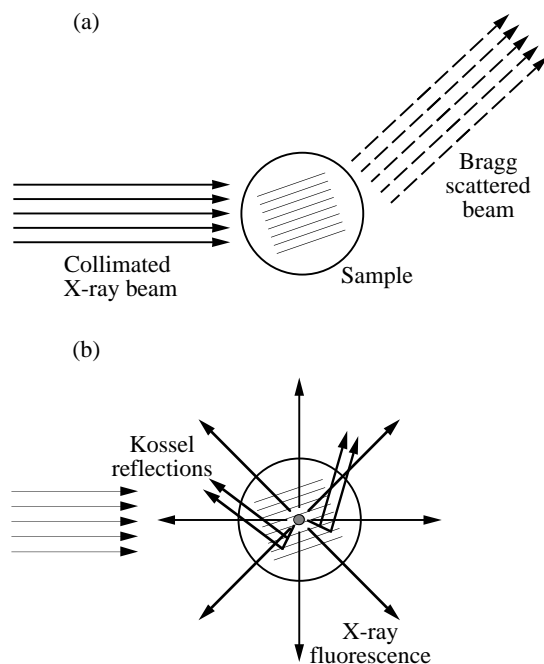


Figure 2. The production of x-ray Kossel lines by fluorescent x-rays. (a) In the usual geometry for x-ray diffraction studies a collimated beam of incident x-rays is used and each set of planes in a Bragg reflecting position gives rise to a narrow parallel diffraction beam. (b) If the wavelength of the incident x-rays is close to an absorption edge of one of the atomic species present in the crystal, fluorescent x-rays are produced. These can be treated as if they arise from a point source at the centre of the crystal. The divergent light gives rise to Kossel lines.

Half a century after their discovery for x-rays, the optical analogues of Kossel lines were observed in studies of the liquid-crystal blue phases [2]. These structures have repeat distances in the visible wavelength range and they selectively reflect light under similar geometrical conditions to those for the Bragg reflection of x-rays from crystal structures. The Kossel lines observed from blue phases have been used primarily in the study of the structural symmetries of these systems [3–5], though quantitative structural measurements have also been made [6].

The optical conditions for the observations of Kossel lines in liquid-crystal systems at visible wavelengths are, unsurprisingly, different from those for the x-ray case. Monochromatic light may be generated using a laser and then made to converge on the liquid-crystal sample using a microscope and a high-numerical-aperture objective. The reflected light may then be collected using the same objective and the Kossel lines observed in the back focal plane as bright lines on a dark background. In this optical arrangement the Kossel lines appear as the projections of circles onto a plane giving either circles, ellipses or straight lines depending on the orientation of the reciprocal-lattice vectors to the viewing direction. The image created by these lines in the back focal plane of the objective is called a Kossel diagram. Each position on the Kossel diagram is directly related to the directional parameters of the collected light, i.e., the incident and azimuthal angle relative to the objective.

In addition to its application to the helicoidal blue phases, the Kossel diagram technique has been used to study aligned samples of chiral nematic liquid crystals [7]. A monodomain sample with the helicoidal axis parallel the microscope axis results in a Kossel diagram consisting of a bright annulus, the width of which is related to the birefringence of the system. The technique can be applied to any helicoidal structure, including chiral smectic phases, though the chiral tilted phases exhibit a more complex optical structure than the chiral nematic phase, so analysis of the Kossel diagrams is correspondingly more complex. Twist grain boundary (TGB) phases form a novel class of smectic phases with helicoidal structures that have been observed in many highly chiral liquid crystals [8, 9]. In the TGB_A phase, screw dislocations occur periodically through the planes of the smectic-A phase, resulting in a helical macrostructure which retains blocks of the smectic-A layered arrangement. The TGB_A phase is the liquid-crystal analogue of the Abrikosov phase [10], and the frustrated structure is usually stable over only a few degrees. There have been rather few discussions of the optical properties of TGB phases [11–13]. This paper reports a study of the optical properties of the TGB_A phase of the liquid-crystal material 14P1M7 [14] (also known as AS425 [14b]) using Kossel diagrams. The Kossel diagrams are used to deduce the handedness of the structure and to determine accurately the pitch variation across the TGB_A phase range.

2. Experimental apparatus

The apparatus used to produce Kossel images in this work has been described previously in several papers [15, 16]. A visible laser diode emitting at a wavelength of 670 nm was used as the light source. The laser was coupled to the reflection arm of a Olympus BHMJ metallurgical reflection microscope. The monochromatic light was focused onto the sample using an Olympus 100 \times oil immersion objective with a numerical aperture of 1.3, allowing a total angular range of incident light of up to 110 $^\circ$ in the sample. In order to maintain the temperature stability of the sample, the objective was also heated using a Linkam TMS90 temperature controller with a stability of ± 0.01 $^\circ\text{C}$. The Kossel diagram image, generated in the back focal plane of the objective, was imaged using a lens and CCD video camera, giving a Kossel diagram image resolution of about 300 \times 300 pixels. The video images were digitized using a frame-grabbing card and image-processing software both installed onto a 486 IBM-compatible personal computer.

The radial position of a point on the Kossel diagram is directly proportional to the sine of the angle at which light enters the objective, even for high-numerical-aperture systems [16]. Hence, direct measurements may be made from the Kossel diagrams. This property was checked and the Kossel diagrams calibrated using a reflecting diffraction grating, having well defined angles of diffraction. Details of the calibration have been given elsewhere [16] and the numerical aperture of the optical system using the 100 \times oil immersion objective was found to

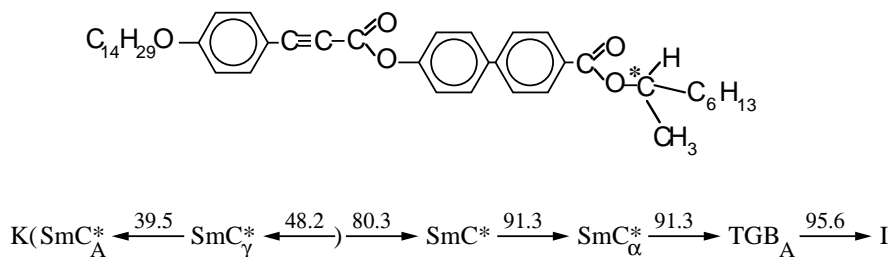


Figure 3. The chemical structure and phase sequence of the compound 14P1M7 [14] used in the experiments. The numbers denote temperatures in degrees centigrade. The brackets and reverse arrows in the phase sequence indicate monotropic phases. SmC_A^* is an antiferroelectric phase, SmC_γ^* is ferrielectric and SmC^* is ferroelectric. The structure of the phase SmC_α^* is still open to question.

be 1.23 ± 0.01 . The material studied here was the compound 14P1M7 [14b] provided by Hull University, shown in figure 3, which exhibits a TGB_A phase below 100°C . This material was chosen for study because of the relatively low temperature at which the TGB_A phase occurs, the upper temperature limit being determined by the temperature to which the objective lens could be heated safely. The slight differences in transition temperatures reported for the material studied here (synthesized with the batch code AS425) and 14P1M7 are attributed to different optical purities of the two batches of the material.

3. Theory of oblique-angle selective reflection from cholesteric helices

The optics of the TGB_A phase has not, at this stage, been completely described theoretically. However, to a first approximation, it seems reasonable to assume that at wavelengths of the same order as the helical pitch (~ 600 nm) the discrete nature of the S_A blocks (~ 20 nm) will not significantly affect the optical properties of the phase. Hence the work carried out in recent years considering the optical properties of the cholesteric phase may be used to describe the essential properties of reflection from the TGB_A phase.

Much of the early work considering the selective reflection of light from cholesteric helices at oblique angles primarily involved computer simulations [17, 18]. However, in more recent work, Oldano and co-workers [19, 20] have derived solutions on a more analytical basis using the fact that the electric field vector of the light in the liquid crystal takes the form of a Bloch wave. Any wave travelling in a periodic medium takes on the periodicity of the medium and is a Bloch wave. Hence, this wave may be considered as an infinite Fourier series. In different papers, Oldano and co-workers determine the coefficients of this Fourier series by either calculating the determinant of an infinite matrix using various approximations, or by considering only the largest components of the Fourier series [21].

To summarize their results, Oldano *et al* find that light of a certain frequency and incidence angle will, in general, excite four modes which represent elliptically polarized light travelling through the medium. However, for each of the modes, one of the other modes differs only in the sign of its wave-vector component along the helical axis. Hence, these two modes are complimentary and only two truly independent modes exist for any specific frequency of light and incidence angle. The wave vectors for these two modes are derived and a number of possibilities found: firstly, both wave vectors are real in which case the two modes propagate without attenuation (figure 4(a)); secondly, one or both wave vectors are complex and the modes are attenuated, corresponding to a reflection of light into the complimentary mode

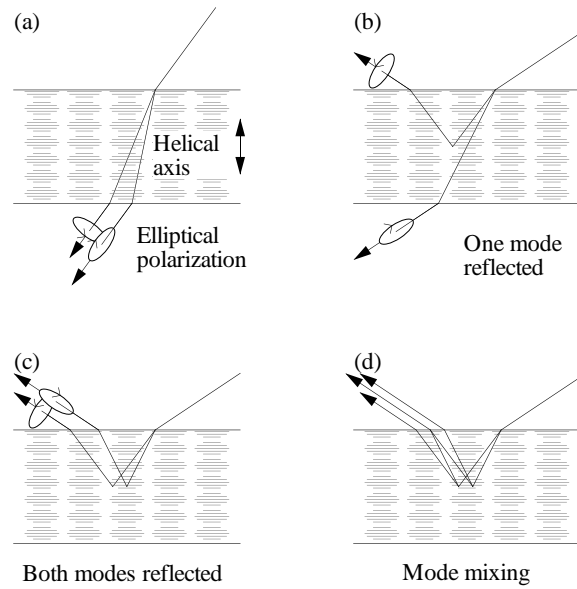


Figure 4. Representation of the various modes that occur in a helicoidal structure.

and fulfilling the Bragg condition (figures 4(b) and 4(c)); finally, both the wave vectors are complex, giving reflection, but the usual Bragg condition is not fulfilled (figure 4(d)), and there is a mixing between the modes.

For the purposes of discussion, a material-independent reduced parameter, m , may be defined for the incidence angle such that

$$m = n_{lc} \sin \theta_{lc} = n_{glass} \sin \theta_{glass} = \dots$$

where n_{lc} and n_{glass} are refractive indices in the liquid crystal and glass slide of the sample cell respectively and θ_{lc} and θ_{glass} are the angles of propagation of the light. For the frequency of the light the situation is more complex. Oldano *et al* define a reduced frequency, ω_r , as

$$\omega_r = \frac{\omega}{2qc} = \frac{p}{2\lambda}$$

where ω is the angular frequency of the light, λ is its wavelength in free space, c is the speed of light, p is the pitch of the helix in the mesophase and q is the chirality. The theoretical behaviour of the solutions of Maxwell's equations in the helicoidal structure may then be summarized by a stability plot, or map of the solutions, illustrating the various optical properties of the helical structure as a function of the reduced parameters (figure 5). Since the Kossel diagram technique exploits monochromatic light incident on the sample from many angles, a radial cross section through the Kossel diagram is directly related to a vertical cross section of the stability plot (the line CD in figure 5). Conversely, a reflection spectrum is equivalent to a horizontal cross section through the stability plot (the line AB in figure 5).

Oldano and co-workers [20] discuss the polarization properties of the modes in some detail. In a previous paper, the various theoretical discussions of selective reflection from chiral nematic liquid crystals were used to explain the polarization-dependent details that were observed in the Kossel diagrams of aligned helicoidal structures [7]. The details are not repeated here, but the Kossel images of aligned chiral nematic samples each comprise a bright annulus with a superimposed dark spiral structure. An intense central ring within

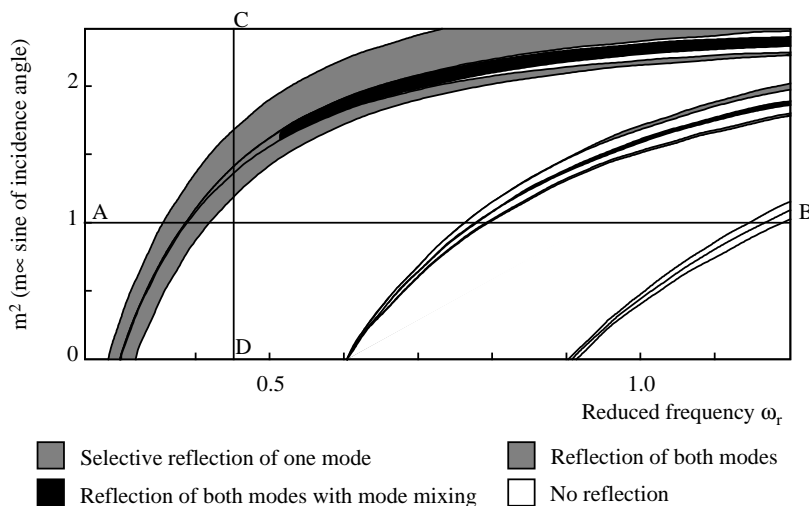


Figure 5. A theoretical stability plot showing the reflection properties of the cholesteric helix as a function of frequency and incidence angle (after Oldano *et al* [19, 20]). The line AB represents a frequency spectrum taken at fixed incidence angle. The line CD represents a radial section through a Kossel diagram image at fixed frequency.

the bright annulus may also be observed when both modes are reflected. The handedness of the spiral pattern observed is related to the chirality of the phase with a right-handed twist resulting in a left-handed spiral pattern. The presence of the more intense central ring and the spiral 'extinction' pattern are in full accordance with the analytical modelling of the selective reflection of cholesteric phases by Oldano *et al*.

4. Results and discussion

The sample of 14P1M7 was placed between glass slides which had been treated with rubbed polyvinyl alcohol (PVA) to promote planar alignment. The PVA alignment causes the helix of the TGB_A phase to align perpendicular to the sample cell surfaces, parallel to the viewing direction. Kossel diagram images, shown in figure 6, were taken at a range of temperatures across the TGB_A phase of 14P1M7. As may be seen from figure 6, the Kossel diagram images consist of annuli, as would be expected for a helicoidal structure aligned along the viewing direction and reflecting the incident light. Comparing the appearance of the Kossel diagrams to that expected from the stability plot (figure 5) it may be seen that the Kossel diagrams correspond to reduced frequencies around $\omega_r \sim 0.4$. In such a comparison, the radial position in the Kossel diagram corresponds to the vertical distance along a line such as CD in figure 5. The dark central region of the Kossel diagram indicates transmission of light by the helicoidal structure. The bright annulus indicates reflection of one or other of the modes, or of both. In figure 6(a), where the central dark region of the Kossel diagram has almost disappeared, $\omega_r \sim 0.3$. Quantitative analysis of the data allows pitch measurements to be determined from the Kossel diagrams, avoiding the dispersion problems associated with such measurements from reflection spectra. This point is considered in more detail below.

Comparing these Kossel diagrams with those of a monodomain chiral nematic liquid crystal, TM533 [7, 22], as shown in figure 7, it can be seen that optics of the TGB_A phase appears to be identical to that of the cholesteric material. Qualitatively, the Kossel diagrams

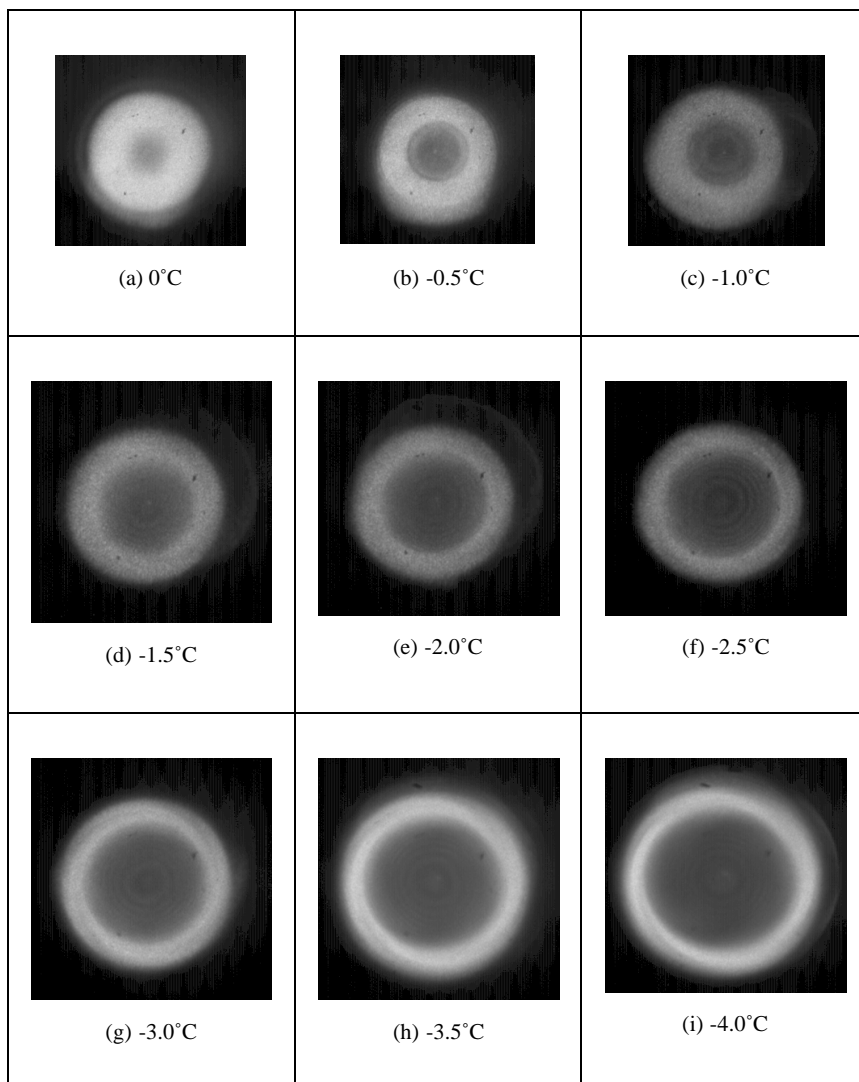


Figure 6. A series of Kossel diagram images taken from the TGB_A phase in 14P1M7 at a range of temperatures from (a) just below the TGB_A -to-isotropic transition to (i) just above the TGB_A -to- SmC^* phase transition in steps of 0.5°C . The images were taken at a wavelength of 670 nm. Notice the spiral bands on the larger annuli.

of figures 6 have poorer contrast than those in figure 7. This is a consequence of the quality of the monodomain sample studied; it is far easier to produce uniform monodomain samples of cholesteric liquid-crystals than of any smectic liquid-crystal phase.

4.1. Kossel diagram reflection band spirals

The superposition of darker spiral bands upon the broad reflection band due to the helicoidal structure of the TGB_A phase is evident in the Kossel diagrams shown in figures 6(f) to 6(i). The spirals display opposite handedness in the TGB_A Kossel diagrams to that in the chiral

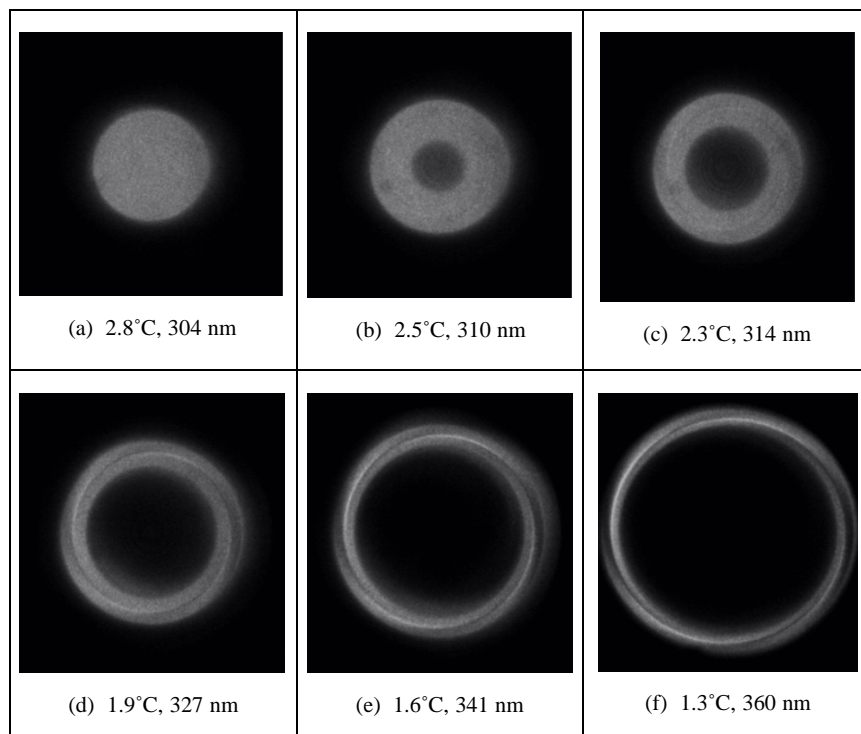


Figure 7. Kossel diagrams of TM533 at a range of temperatures above the phase transition from the smectic-A to the cholesteric phase. Below each image, the temperature above this phase transition is shown, together with the helicoidal pitch measured from the reflection spectra at normal incidence. The Kossel diagrams were recorded with 488 nm light.

nematic system (figures 7(d)–7(f)). It can be concluded from direct observation that 14P1M7 has a left-handed helicoidal structure across the TGB_A phase, while TM533 has a right-handed helicoidal structure. Srajer *et al* [14a], report 14P1M7 to have a right-handed TGB_A structure, though contact measurements [24] confirm the result of a left-handed structure for this system, deduced from the Kossel diagrams. No spirals are observed in figures 6(a)–6(e) or 7(a)–7(c) since the structures in those cases reflect almost completely circularly polarized light. The ellipticity of the polarization, which gives rise to the observation of the spiral structure, becomes more pronounced as ω_r increases.

4.2. Pitch measurements from Kossel diagrams

The form of the Kossel diagram obtained from a helical structure such as the TGB_A or cholesteric phases depends directly on the helical pitch, the refractive indices and the wavelength of the light used. The Kossel diagrams can therefore be used to deduce various physical properties of the system, including the helicoidal pitch. The advantages of using this technique for measuring the helical pitch include the possibility of probing beyond the visible wavelength range and not having measurements distorted by the natural dispersion of the material.

The way in which pitch measurements may be made from the Kossel diagrams has been described in detail elsewhere [7]. The reflected light obeys Bragg's law for reflections either

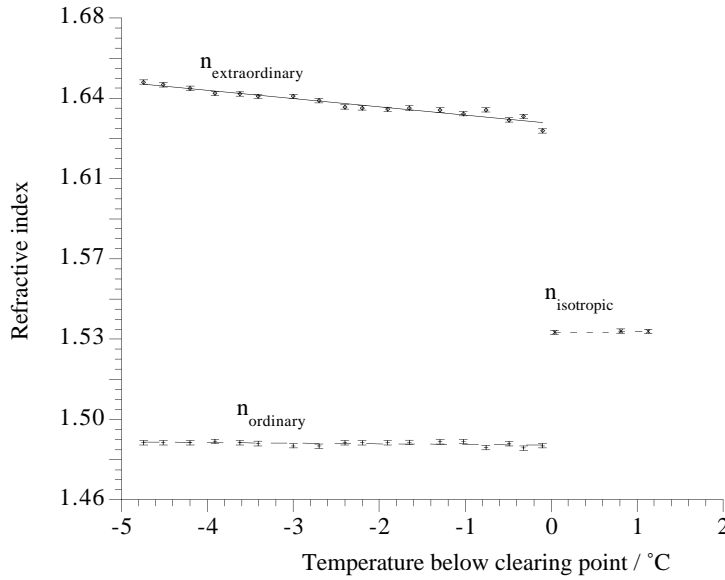


Figure 8. The refractive indices of 14P1M7 as a function of temperature in the TGB_A phase.

at normal incidence or for the ordinary ray. In terms of the parameters employed in this paper, Bragg's law may be written as

$$n \cos \theta = \frac{1}{\omega_r}$$

where n is the refractive index of the material, θ is the angle of light propagation with respect to the layer normal and ω_r is as defined previously. Substituting in

$$\cos \theta = \sqrt{1 - \sin^2 \theta} \quad \text{and} \quad m = n \sin \theta$$

leads to equation (1):

$$m^2 = n^2 - \frac{1}{4\omega_r^2} = n^2 - \frac{\lambda^2}{p^2}. \quad (1)$$

The parameter m can be measured directly from the Kossel diagrams, once the images have been calibrated. The inner edge of the annulus is the one chosen for the measurements as then n is n_o , the ordinary refractive index, and equation (1) is exact. The situation at the outer edge of the annulus is more complicated as the extraordinary ray does not obey Bragg's law. Equation (1) was used to derive pitch measurements in the TGB_A phase of 14P1M7 from the Kossel diagrams. The refractive indices of 14P1M7 were found to within 0.5% from the angle of total internal reflection of monochromatic light from an aligned sample held between two glass prisms. The temperature was controlled to ± 0.1 °C and the data are presented in figure 8. The variation of the refractive indices is almost linear across the temperature range of the TGB_A phase and there is no evidence of any pretransitional phenomena.

Figure 9 shows the pitch measurements deduced from measurements of the position of the inner edge of the Kossel diagrams and n_o . The graph illustrates that the TGB_A phase pitch varies by approximately 20% across the 4.2 K temperature range of the phase. Evidence of slight pretransitional divergence in the pitch may be seen near the transitions to both the SmC_α^* phase and the isotropic phase, though in general the dependence is approximately linear. The

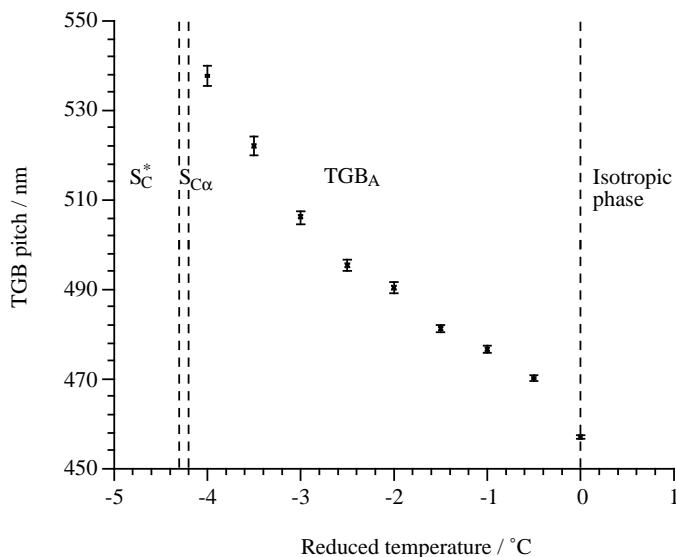


Figure 9. The pitch of the TGB_A phase deduced from measurements of the inner edges of the annuli (figure 6) and the refractive index (figure 8) across the temperature range of the phase.

absolute values of the pitch are similar to those reported for other TGB_A systems [12, 13], though the uncertainties quoted here are significantly smaller than those in reference [12]. The data presented in figure 9 can be compared with the pitch measurements reported by Srajer *et al* [14a] who also studied 14P1M7. Their pitch measurements were deduced from selective-reflection data and an assumption of the average refractive index of the material as approximately 1.6. The measurements reported here agree qualitatively with those in reference [14a], being approximately linear with temperature, though they differ in their absolute value and in the slight pretransitional phenomena observed in figure 9. We believe that the difference in the absolute value of the pitch may be attributed to the differing optical purities of the different batches of the material studied, since previous measurements on chiral nematic materials [7] have confirmed the validity of this technique of measuring pitch. The slight pretransitional divergence observed here is a result of using the temperature-dependent refractive index values in deducing the pitch and so would not be observed in data derived from temperature-independent values of refractive index.

5. Conclusions

Spiral features identical to those reported for a chiral nematic material have been observed in the Kossel diagrams of a TGB_A phase, confirming the identical optical properties of the two mesophases. The handedness of the spiral pattern was employed to deduce that 14P1M7 has a left-handed helicoidal structure in the TGB_A phase. Pitch measurements were made from the Kossel diagrams of the system by considering the position of the inner edge of the Kossel annulus. The advantages of this method of deducing the pitch over measurements made from selective-reflection spectra [23] include the fact that only one refractive index needs to be measured, and that the use of monochromatic light ensures that no dispersion effects occur. Furthermore, measurements of the pitch from selective-reflection spectra suffer from experimental error introduced because the light is generally not at normal incidence, a factor

which does not contribute here. The pitch of the TGB_A phase was observed to increase as the temperature decreases and, though the variation was approximately linear, the accurate pitch measurements presented allow us to conclude some evidence of pretransitional divergence close to the bounding phase transitions, not previously remarked upon.

Acknowledgments

The authors thank the EPSRC and MOD for financial support (grant GR/H/95860) and William Deakin for useful and enthusiastic discussions.

References

- [1] Kossel W, Loeck V and Voges H 1935 *Z. Phys.* **94** 139
- [2] Cladis P E, Garel T and Pieranski P 1986 *Phys. Rev. Lett.* **57** 2841
- [3] Meiboom S and Sammon M 1981 *Phys. Rev. A* **24** 468
- [4] Johnson D L, Flack J H and Crooker P P 1980 *Phys. Rev. Lett.* **45** 641
- [5] Heppke G, Jerome R, Kitzerow H S and Pieranski P 1989 *J. Physique* **50** 549
- [6] Miller R J, Gleeson H F and Lydon J E 1996 *Phys. Rev. Lett.* **77** 857
- [7] Miller R J, Gleeson H F and Lydon J E 1999 *Phys. Rev. E* **59** at press
- [8] Goodby J W, Waugh M A, Stein S M, Chin K, Pindak R and Patel J S 1989 *J. Am. Chem. Soc.* **111** 8119
- [9] Slaney A J and Goodby J W 1991 *Liq. Cryst.* **9** 849
- [10] Ihn K J, Zasadzinski J A N, Pindak R, Slaney A and Goodby J 1992 *Science* **258** 275
- [11] Navailles L, Nguyen H T, Barois P, Isaert N and Delord P 1996 *Liq. Cryst.* **20** 653
- [12] Ribeiro A C, Oswald L, Nicoud J F, Guillon D and Galerne Y 1998 *Eur. Phys. J. B* **1** 503
- [13] Isaert N, Navailles L, Barois P and Nguyen H G 1994 *J. Physique II* **4** 1501
- [14a] Srajer G, Pindak R, Waugh M A, Goodby J W and Patel J S 1990 *Phys. Rev. Lett.* **64** 1545
- [14b] Robinson W K, Miller R J, Gleeson H F, Hird M, Seed A J and Styring P 1996 *Ferroelectrics* **180** 291
- [15] Miller R J and Gleeson H F 1995 *Phys. Rev. E* **52** 5011
- [16] Miller R J and Gleeson H F 1996 *J. Physique II* **6** 909
- [17] Berreman D W 1972 *J. Opt. Soc. Am.* **62** 502
- [18] Dreher R and Meier G 1973 *Phys. Rev. A* **8** 1616
- [19] Oldano C, Miraldi E and Taverna Valabrega P 1983 *Phys. Rev. A* **27** 3291
- [20] Miraldi E, Oldano C, Taverna Valabrega P and Trossi L 1983 *Mol. Cryst. Liq. Cryst.* **103** 155
- [21] Oldano C 1985 *Phys. Rev. A* **31** 1014
- [22] Nomenclature of Merck Limited, Merck House, Poole, Dorset, UK.
- [23] Gleeson H F and Coles H J 1989 *Mol. Cryst. Liq. Cryst.* **170** 9
- [24] Miller R J 1994 *PhD Thesis* Manchester University